Dyes and Pigments 101 (2014) 30–37

Contents lists available at ScienceDirect

Dyes and Pigments

journal homepage: www.elsevier.com/locate/dyepig

A novel Zn^{2+} complex as the ratiometric two-photon fluorescent probe for biological Cd^{2+} detection

Weipeng Ye [a], Shuxing Wang [a], Xiangming Meng [a,*], Yan Feng [a], Hongting Sheng [a], Zonglong Shao [a], Manzhou Zhu [a,*], Qingxiang Guo [b]

[a] School of Chemistry and Chemical Engineering, Anhui University, 230601 Hefei, PR China
[b] Department of Chemistry, University of Science and Technology, Hefei 230026, PR China

ARTICLE INFO

Article history:
Received 14 June 2013
Received in revised form
30 August 2013
Accepted 10 September 2013
Available online 27 September 2013

Keywords:
Ratiometic
Two-photon
Fluorescent probe
Zn^{2+} complex
Cd^{2+}
Bio-imaging

ABSTRACT

A novel Zn^{2+} complex as the ratiometric two-photon fluorescent probe (**HQZn**) for Cd^{2+} detection was synthesized. Fluorescence emission spectra of the probe showed a large red-shift (75 nm) and obvious enhancement of fluorescent intensity upon the addition of Cd^{2+}. **HQZn** shows high selectivity for Cd^{2+} over other metal ions, and can eliminate the interference of Zn^{2+} during Cd^{2+} detection. Maldi-TOF MS spectra indicated that the response of **HQZn** to Cd^{2+} was caused by central metal displacement. Cell cytotoxicity and bio-imaging studies revealed that **HQZn** was cell-permeable and it could be used to detect intracellular Cd^{2+} with low cytotoxicity under two-photon excitation.

1. Introduction

Cadmium, as one of the most toxic metal pollutant, can accumulate in the human body for more than 10 years and cause many serious diseases, such as renal dysfunction, calcium metabolism disorders, prostate cancer, etc. [1,2]. Therefore, detection and quantification of Cd^{2+} in vitro and in vivo is highly needed.

Fluorescent probes have been regarded as the most powerful tools for monitoring metal ions in biological and environmental samples for their high selectivity and sensitivity [3–6]. Many fluorescent probes for Cd^{2+} have been reported, and most of them were "off-on" type [7–13]. Detecting Cd^{2+} depended on the change of the emission at only one wavelength, which may cause difficulty in quantitative determination and bio-imaging due to the background interference (pH, polarity, temperature, and so forth) [14–17]. Ratiometric probes can overcome these limitations because of their self-calibration by measuring the ratio of emission at two different wavelengths. Recently, two-photon microscopy (TPM) has been evolved into a widely used tool in biomedical research for its evident advantages over one-photon microscopy (OPM), including increased penetration depth, localized excitation and prolonged observation time [18–21]. Many two-photon fluorescent probes have been developed for detecting various metal ions, while two-photon probes for Cd^{2+} (especially ratiometric) have rarely been reported [22,23].

Although Zn^{2+} and Cd^{2+} belong to the same group, they play totally different roles in biochemical processes. Cd^{2+} can replace Zn^{2+} in many zinc enzymes, thereby impairing their catalytic activities [24]. So far, most of the reported fluorescent probes for Cd^{2+} suffered from the interference from Zn^{2+}, which can be ascribed to highly similar chemical properties of Zn^{2+} and Cd^{2+} [25–30]. Therefore, it is still a challenging task to develop highly selective fluorescent probes for Cd^{2+}, especially avoiding the interference of Zn^{2+} in detection. Previous reported results indicated that Cd^{2+} can displace Zn^{2+} in its complex and give different emission fluorescence due to their different coordination mode [31]. Thus we ask an interesting question whether or not we can detect Cd^{2+} based on a Zn^{2+} complex by central metal displacement. If our goal can be achieved, we will eliminate the Zn^{2+} interference during Cd^{2+} detection. Inspired by this idea and our recent success in developing two-photon probes for Cd^{2+} and Zn^{2+} based on 6-substituted quinoline skeletons [32–34], we designed a 6-substituted quinoline Zn^{2+} complex (**HQZn**, Scheme 1) as the ratiometric two-photon fluorescent probe for Cd^{2+}. Maldi-TOF MS spectra was

* Corresponding authors. Tel./fax: +86 551 63861467.
E-mail addresses: mengxm@ahu.edu.cn (X. Meng), zmz@ahu.edu.cn (M. Zhu).

0143-7208/$ – see front matter © 2013 Elsevier Ltd. All rights reserved.
http://dx.doi.org/10.1016/j.dyepig.2013.09.013

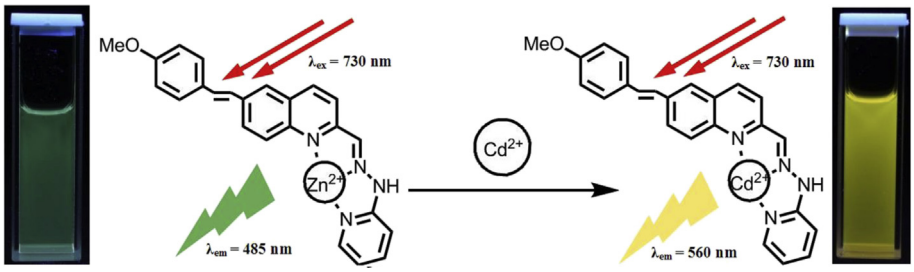

Scheme 1. The design of **HQZn** for Cd^{2+} detection.

used to reveal that the response of **HQZn** to Cd^{2+} was caused by central metal displacement. Meanwhile, cell cytotoxicity and bio-imaging studies indicated that **HQZn** was cell-permeable and it could be used to detect intracellular Cd^{2+} with low cytotoxicity under two-photon excitation.

2. Experimental section

2.1. Materials and physical measurements

All reagents were commercially purchased, and the solvents were used after appropriate distillation or purification. The solutions of metal ions were prepared from chloride salts. HEPES buffer solutions (20 mM, pH 7.4) were prepared in water. ^{1}H NMR spectra were recorded on Bruker-400 MHz spectrometers and ^{13}C NMR spectra were recorded on 100 MHz spectrometers. All solvents used in the test were chromatographically pure. UV–vis absorption spectra were recorded on a Tech-comp UV 1000 spectrophotometer. Fluorescence spectra were recorded on a HITACHIF-2500 spectrometer. MS spectra were recorded on a Bruker autoflex III MALDI-TOF mass spectrometer. Cells imaging was carried out on a Zeiss LSM 510 Meta NLO confocal microscope.

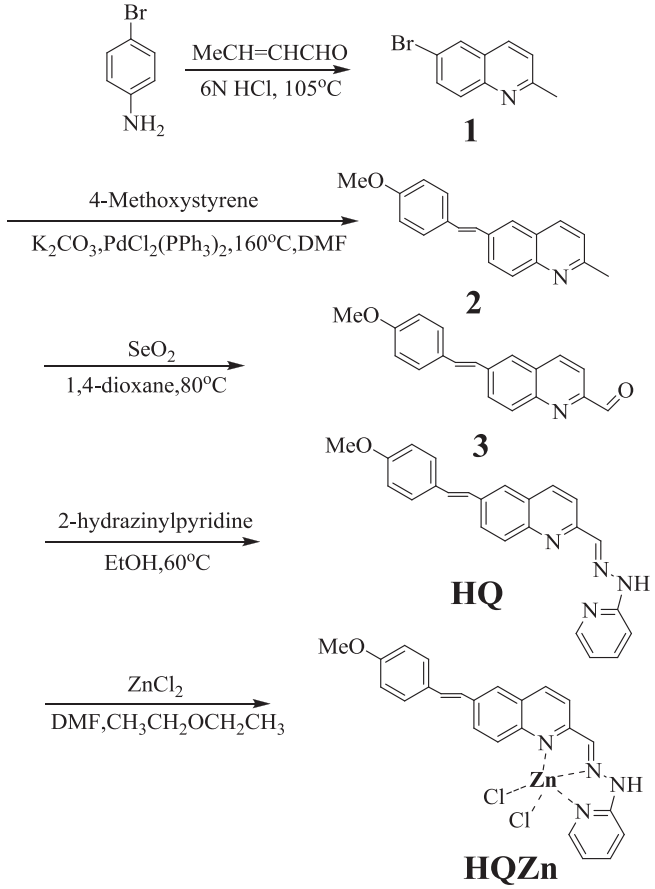

Scheme 2. Synthetic route of **HQZn**.

2.2. Synthesis procedure

2.2.1. 6-bromo-2-methylquinoline (*1*)

A mixture of 4-bromobenzenamine (14.59 g, 84.8 mmol) and HCl (6 N, 60 mL) was heated to 100 °C, then crotonaldehyde (11.9 g, 170 mmol) was added slowly. The resulting mixture was refluxed until TLC shows no raw material exists. After cooling to room temperature, 200 mL H_2O was added and the mixture was extracted with EtOAc (100 mL × 2) to remove the unreacted crotonaldehyde. The aqueous phase was neutralized with ammonia water and then extracted with EtOAc (50 mL × 2). The organic phase was dried over anhydrous Na_2SO_4 and evaporated to give crude residue. The crude product was recrystallized in EtOAc/PE to give 13.46 g of **1** (60.64 mmol, 75.6%). ^{1}H NMR (400 MHz, $CDCl_3$, ppm): δ 2.73 (3H, s), 7.29–7.31 (1H, d, J = 8.4 Hz), 7.73–7.75 (1H, d, J = 9.0 Hz), 7.87–7.96 (3H, m). ^{13}C NMR (100 MHz, $CDCl_3$, ppm): δ 25.18, 119.57, 122.91, 127.64, 129.54, 130.12, 133.03, 135.49, 146.05, 159.45.

2.2.2. (E)-6-(4-methoxystyryl)-2-methylquinoline (*2*)

A mixture of **1** (6.03 g, 27.15 mmol), 4-methoxystyrene (4.37 g, 32.58 mmol), $PdCl_2(PPh_3)_2$ (77 mg, 0.97 mmol), K_2CO_3 (11 g, 79.7 mmol) and DMF (25 mL) was heated at 160 °C for 24 h [35]. After cooling to room temperature, the mixture was filtered to remove salts, and then 100 mL H_2O was added. The result mixture was extracted by DCM (50 mL × 3). The organic phase was dried over anhydrous Na_2SO_4 and evaporated to give crude residue. The crude product was recrystallized in EtOAc/PE to give 6.77 g of **2** (24.63 mmol, 90.72%). ^{1}H NMR (400 MHz, $CDCl_3$, ppm): δ 2.75 (3H, s), 3.84 (3H, s), 6.91–6.93 (2H, d, J = 8.6 Hz), 7.08–7.21 (2H, q, J = 16.3 Hz), 7.25–7.27 (1H, d, J = 8.3 Hz), 7.48–7.50 (2H, d, J = 8.6 Hz), 7.73 (1H, s), 7.91–7.93 (1H, d, J = 8.9 Hz), 8.01–8.03 (2H, d, J = 8.5 Hz). ^{13}C NMR (100 MHz, $CDCl_3$, ppm): δ 25.11, 55.35,

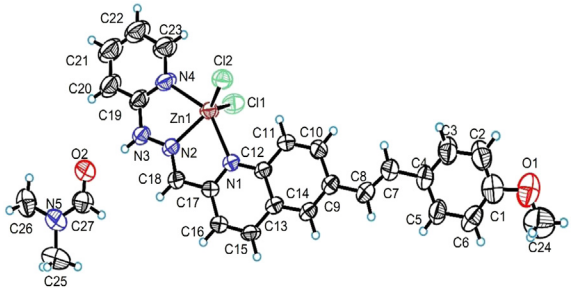

Fig. 1. X-ray crystal structure for **HQZn**.

Table 1
Crystallographic data for **HQZn**.

Compound	HQZn
Chemical formula	$C_{27}H_{27}Cl_2N_5O_2Zn$
Formula mass	589.81
Crystal system	Monoclinic
a/Å	13.8914(5)
b/Å	11.0111(5)
c/Å	20.4872(7)
α/°	90
β/°	105.874(4)
γ/°	90
Unit cell volume/Å^3	3014.2(2)
Temperature/K	291(2)
Space group	P 21/n
Z	4
Number of reflections measured	16,466
Number of independent reflections	4815
R_{int}	0.0407
Final R_1 values ($I > 2\sigma(I)$)	0.0560
Final $wR(F^2)$ values ($I > 2\sigma(I)$)	0.1545
Final R_1 values (all data)	0.0796
Final $wR(F^2)$ values (all data)	0.1702

114.23, 122.39, 125.19, 125.79, 126.81, 127.39, 127.87, 128.59, 129.36, 129.90, 135.26, 136.35, 147.07, 158.43, 159.54.

2.2.3. (E)-6-(4-methoxystyryl)quinoline-2-carbaldehyde (**3**)

A solution of **2** (2.00 g, 7.27 mmol) in dioxane (20 mL) was heated to 60 °C, and SeO_2 (8.00 mmol, 0.889 g) was added to this solution. The reaction temperature was kept at 80 °C for 2.5 h, then the mixture was cooled to room temperature. Precipitates were filtered off and washed with dioxane (5 mL × 2). The organic phase was combined and concentrated to give a crude product. The crude material was purified by column chromatography (DCM as the eluent) to give 1.818 g of **3** (6.61 mmol, 90.9%). ^{1}H NMR (400 MHz, $CDCl_3$, ppm): δ 3.85 (3H, s), 6.92–6.94 (2H, d, J = 8.6 Hz), 7.11–7.30 (2H, dd, J = 16.1 Hz), 7.50–7.52 (2H, d, J = 8.6 Hz), 7.82 (1H, s), 7.99–8.05 (2H, dd, J = 16.4 Hz), 8.18–8.25 (2H, dd, J = 18.1 Hz), 10.21 (1H, s). ^{13}C NMR (100 MHz, $CDCl_3$, ppm): δ 55.37, 114.33, 117.88, 125.11, 125.15, 128.19, 128.30, 129.41, 130.54, 130.64, 131.37, 136.97, 138.71, 147.44, 151.91, 159.97, 193.51.

2.2.4. (E)-6-(4-methoxystyryl)-2-(2-(pyridin-2-yl)hydrazono) quinoline (**HQ**)

A mixture of **3** (0.5 g, 1.73 mmol) and 2-hydrazinylpyridine (0.22 g, 2.07 mmol) in ethanol (10 mL) was heated to 60 °C. The reaction temperature was kept at 60 °C for 0.5 h. After cooling to room temperature, precipitates were collected by filtration and recrystallized in EtOH to give 0.56 g of **HQ** (1.42 mmol, 80%). ^{1}H NMR (400 MHz, DMSO-d_6, ppm): δ 3.80 (3H), 6.92–6.94 (3H), 7.27–7.49 (2H), 7.60–7.63 (2H), 7.71–8.05 (3H), 8.07–8.12 (2H), 8.18–8.31 (2H), 8.49–8.56 (1H), 10.95–15.28 (1H).

2.2.5. Zinc(II) complex of HQ (**HQZn**)

HQ (120 mg, 0.3 mmol) and $ZnCl_2$ (0.04 g, 0.3 mmol) were dissolved in 4 mL DMF and stirred for 2 h at room temperature, then 2 mL Et_2O was added. Orange acicular single crystals were obtained at room temperature after a few days. ^{1}H NMR (400 MHz, DMSO-d_6, ppm): δ 3.80 (3H), 6.97–7.11 (3H), 7.27–7.34 (1H), 7.35–7.45 (1H), 7.7–8.1 (4H), 8.15–8.37 (2H), 8.45–8.85 (2H), 12.80–15.95 (1H).

2.3. X-ray crystallography

X-ray diffraction data of **HQZn** single crystals were collected on a Siemens Smart 1000 CCD diffractometer. The determination of unit cell parameters and data collections were performed with Mo $K\alpha$ radiation (λ = 0.71073 Å). Unit cell dimensions were obtained with least-squares refinements, and all structures were solved by direct methods using SHELXS-97 [36]. The other non-hydrogen atoms were located in successive difference Fourier syntheses. The final refinement was performed by using full-matrix least-squares methods with anisotropic thermal parameters for non-hydrogen atoms on F^2. The hydrogen atoms were added theoretically and rode on the concerned atoms.

2.4. Preparation of fluorescent titration

Inorganic salt was dissolved in distilled water to afford 10 mM aqueous solution. The 1 mM stock solution of **HQZn** was prepared in absolute methanol. All the measurements were carried out according to the following procedure. To 10 mL volumetric flask containing 250 μL of the solution of **HQZn**, different amounts (25 μL–1000 μL) of metal ions were added directly with micropipette, then diluted with buffered (pH 7.4, 20 mM HEPES) solution. For the Job's plot experiment, **HQZn** (1 mM) in absolute methanol and $CdCl_2$ (1 mM) in distilled water were prepared as stock solutions. The methanol–water solution (3:7, v/v, 20 mM HEPES buffer, pH = 7.4) was prepared. The concentrations of **HQZn** and Cd^{2+} solution were varied, but the total volume was fixed at 10 mL and the total concentrations of **HQZn** and Cd^{2+} are 25 μM. After the mixture was shaken, the maximum of fluorescence intensity was recorded. Fluorescence measurements were carried out with excitation and emission slit width of 10 and 10 nm and PMT Voltage and excitation wavelength was 400 V and 400 nm, respectively.

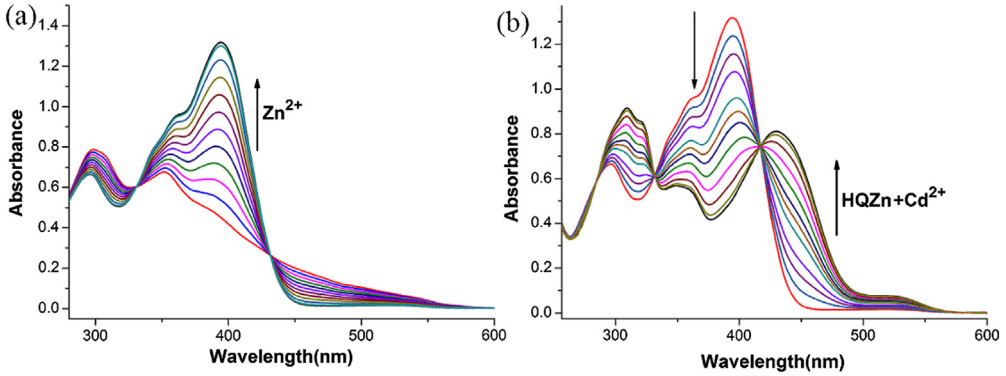

Fig. 2. (a) UV–vis spectra of **HQ** (25 μM) upon the titration of Zn^{2+} (0, 0.1, 0.2, 0.3, 0.4, 0.5, 0.6, 0.7, 0.8, 0.9, 1.0, 1.2 equiv) in the methanol–water solution (3:7, v/v, 20 mM HEPES buffer, pH = 7.4). (b) UV–vis spectra of **HQZn** (25 μM) upon the titration of Cd^{2+} (0, 0.1, 0.2, 0.3, 0.4, 0.5, 0.6, 0.7, 0.8, 0.9, 1.0, 1.2 equiv) in the methanol–water solution (3:7, v/v, 20 mM HEPES buffer, pH = 7.4).

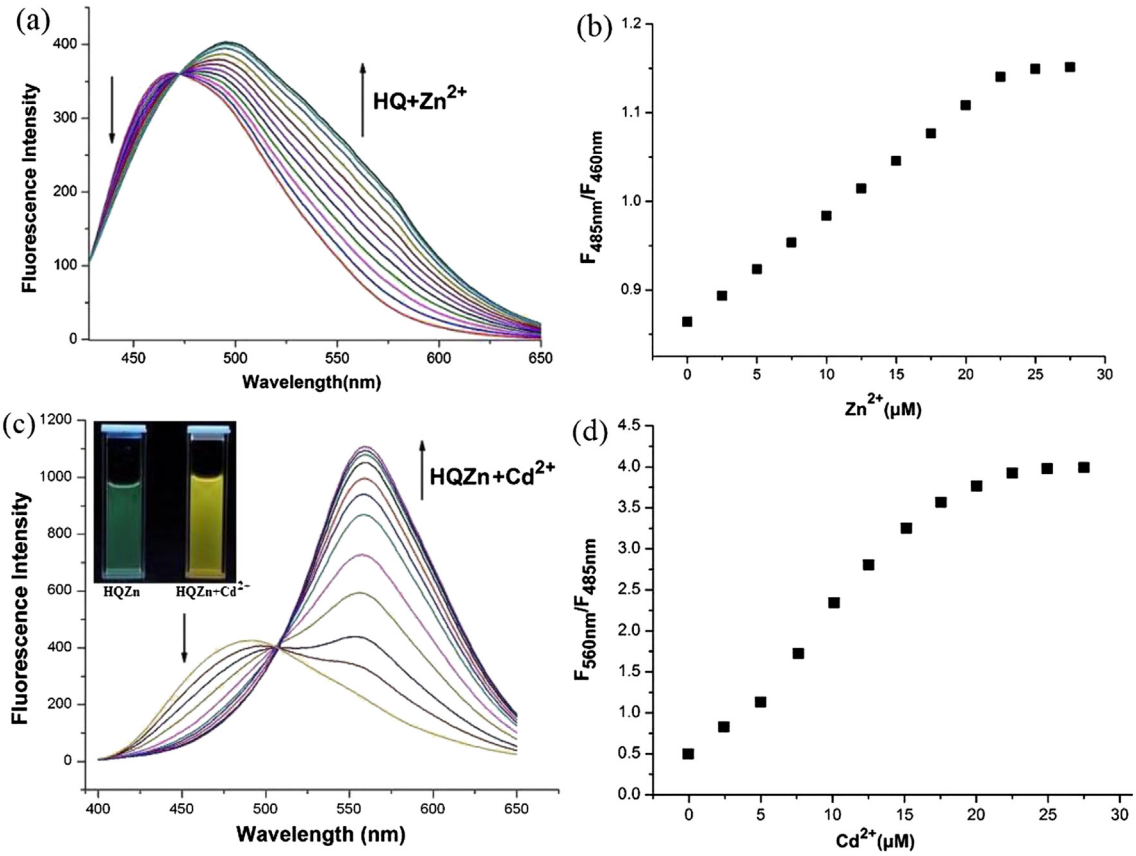

Fig. 3. (a) Fluorescence responses (λ_{ex} = 360 nm) of **HQ** (25 μM) upon the titration of Zn^{2+} (0, 0.1, 0.2, 0.3, 0.4, 0.5, 0.6, 0.7, 0.8, 0.9, 1.0, 1.2 equiv) in the methanol–water solution (3:7, v/v, 20 mM HEPES buffer, pH = 7.4). (b) Ratiometric calibration curve ($F_{485\ nm}/F_{460\ nm}$) as a function of the Zn^{2+} concentration. (c) Fluorescence responses (λ_{ex} = 400 nm) of **HQZn** (25 μM) upon the titration of Cd^{2+} (0, 0.1, 0.2, 0.3, 0.4, 0.5, 0.6, 0.7, 0.8, 0.9, 1.0, 1.2 equiv) in the methanol–water solution (3:7, v/v, 20 mM HEPES buffer, pH = 7.4). Inset: Digital photographs of **HQZn** and **HQZn** in presence of equivalent amount of Cd^{2+} under a hand-held UV–vis (365 nm) lamp. (d) Ratiometric calibration curve ($F_{560\ nm}/F_{485\ nm}$) as a function of the Cd^{2+} concentration.

2.5. Measurement of two-photon absorption cross section (δ)

Two-photon excitation fluorescence (TPEF) spectra were measured using femtosecond laser pulse and Ti: sapphire system (680–1080 nm, 80 MHz, 140 fs, Chameleon II) as the light source. All measurements were carried out in air at room temperature.

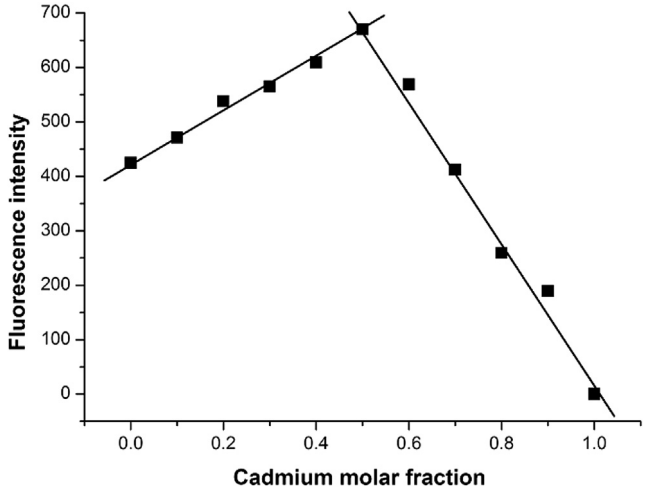

Fig. 4. Job's plot of **HQZn** and Cd^{2+} (λ_{ex} = 400 nm, λ_{em} = 560 nm). The total concentrations of **HQZn** and Cd^{2+} are 25 μM. The experiments were measured at room temperature in the methanol–water solution (3:7, v/v, 20 mM HEPES buffer, pH = 7.4).

Two-photon absorption cross sections were measured using two-photon-induced fluorescence measurement technique. The two-photon absorption cross sections (δ) were determined in CH_3OH by comparing their TPEF to that of fluorescein according to the literature [37].

2.6. Cytotoxicity assays

MTT (5-dimethylthiazol-2-yl-2,5-diphenyltetrazolium bromide) assay was performed as previously reported to test the cytotoxic effect of the probe in cells [32]. HeLa cells were passed and plated to ca. 70% confluence in 96-well plates 24 h before treatment. Prior to **HQZn** treatment, DMEM (Dulbecco's Modified Eagle Medium) with 10% FCS (Fetal Calf Serum) was removed and replaced with fresh DMEM, and aliquots of **HQZn** stock solutions (5 mM DMSO) were added to obtain final concentrations of 10, 30, and 50 μM respectively. The treated cells were incubated for 24 h at 37 °C under 5% CO_2. Subsequently, cells were treated with 5 mg/mL MTT (40 μL/well) and incubated for an additional 4 h (37 °C, 5% CO_2). Then the cells were dissolved in DMSO (150 μL/well), and the absorbance at 570 nm was recorded. The cell viability (%) was calculated according to the following equation: Cell viability% = OD_{570}(sample)/OD_{570}(control) × 100, where OD_{570}(sample) represents the optical density of the wells treated with various concentration of **HQZn** and OD_{570}(control) represents that of the wells treated with DMEM containing 10% FCS. The percent of cell survival values is relative to untreated control cells.

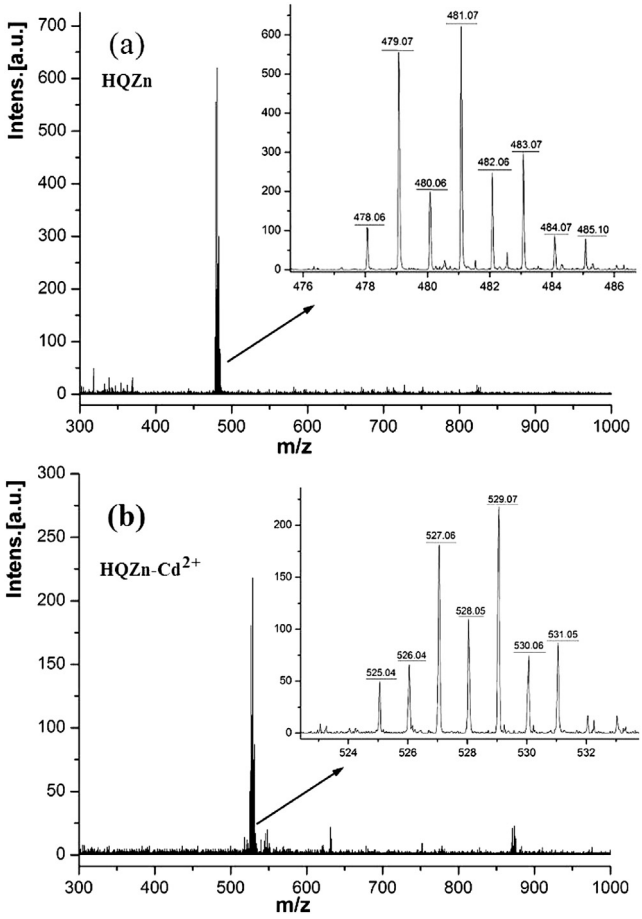

Fig. 5. (a) MALDI-TOF MS spectrum of **HQZn** (DCTB as matrix). (b) MALDI-TOF MS spectrum of **HQZn**–$\mathbf{Cd^{2+}}$ complex (DCTB as matrix).

2.7. Cell culture and two-photon fluorescence microscopy imaging

For two-photon bio-imaging, HeLa cells were cultured in DMEM supplemented with 10% FCS, penicillin (100 μg/mL), and streptomycin (100 μg/mL) at 37 °C in a humidified atmosphere with 5% CO_2 and 95% air. Cytotoxicity assays show that **HQZn** is safe enough for two-photon bio-imaging at low concentrations, so that the cells were incubated with 15 μM **HQZn** at 37 °C under 5% CO_2 for 30 min, washed once and bathed in DMEM containing no FCS prior to imaging. Then 30 μM Cd^{2+} was added in the growth medium for 0.5 h at 37 °C, washed 3 times with PBS buffer. Cells imaging was carried out on a confocal microscope (Zeiss LSM 510 Meta NLO). Two-photon fluorescence microscopy images of labeled cells were obtained by exciting the probe with a mode-locked titanium-sapphire laser source set at wavelength 730 nm.

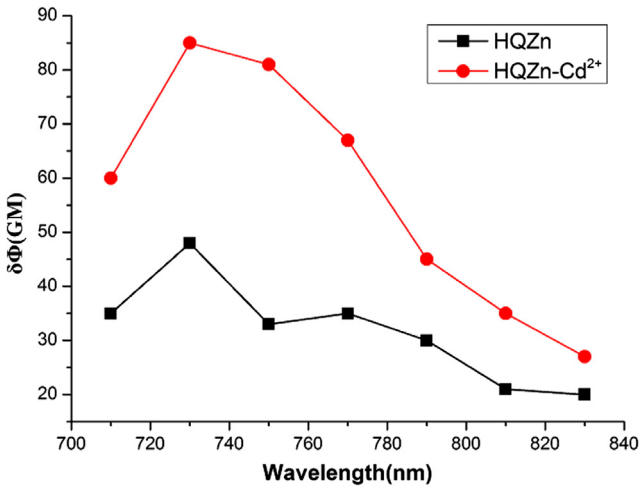

Fig. 6. Two-photon absorption cross sections of **HQZn** and **HQZn**–$\mathbf{Cd^{2+}}$ in CH_3OH under different exciting wavelengths of identical energy of 0.300 w ($c = 1.0 \times 10^{-3}$ mol/L).

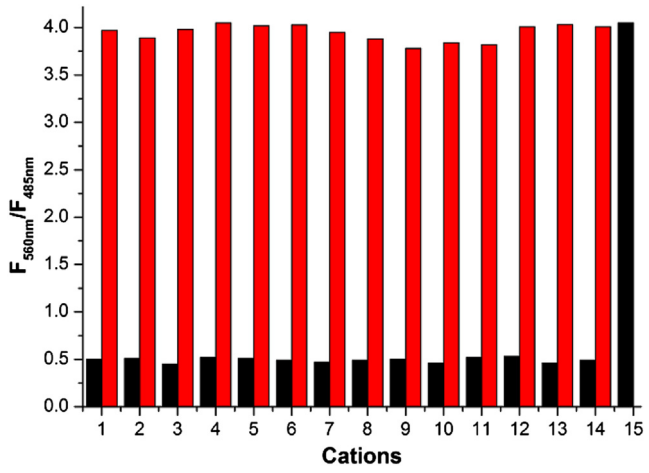

Fig. 7. Ratio ($F_{560\ nm}/F_{485\ nm}$) of **HQZn** upon addition of various metal ions (1–15: Na^+, Ag^+, Mn^{2+}, Cu^{2+}, Hg^{2+}, Pb^{2+}, Mg^{2+}, Ca^{2+}, Fe^{2+}, Co^{2+}, Ni^{2+}, Cr^{3+}, Fe^{3+}, Zn^{2+}, Cd^{2+}) in the methanol–water solution (3:7, v/v, 20 mM HEPES buffer, pH = 7.4, λ_{ex} = 400 nm). The black bars represent the emission of **HQZn** in the presence of 1 equiv of different metal cations to **HQZn**. The red bars represent the change in integrated emission that occurs upon subsequent addition of 1 equiv of Cd^{2+} to the solution (λ_{ex} = 400 nm). (For interpretation of the references to color in this figure legend, the reader is referred to the web version of this article).

3. Results and discussion

3.1. Structure of *HQZn* and *HQZn*–Cd^{2+}

As shown in Scheme 2, the probe **HQZn** was synthesized via five steps from readily available 4-bromoaniline with overall yield of

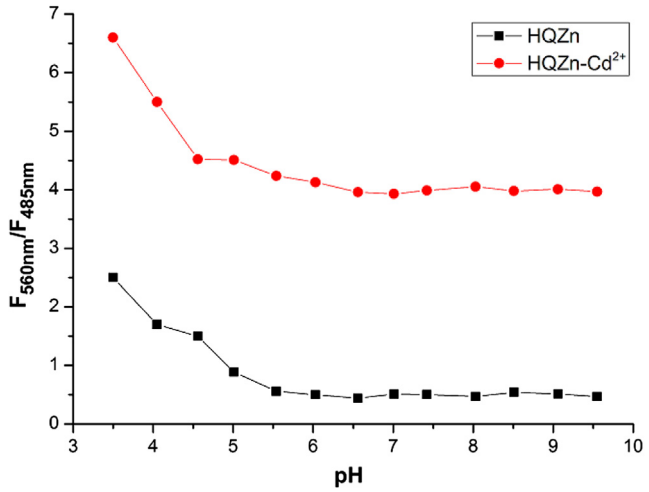

Fig. 8. Ratio ($F_{560\ nm}/F_{485\ nm}$) of **HQZn** and **HQZn**–$\mathbf{Cd^{2+}}$ at various pH values in the methanol–water solution (3:7, v/v, 20 mM HEPES buffer, λ_{ex} = 400 nm).

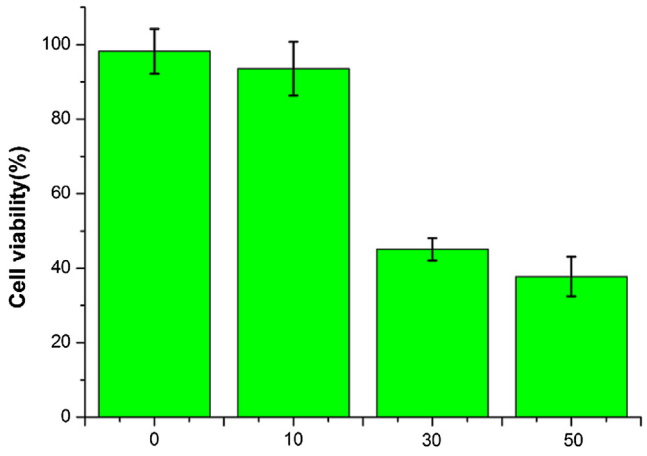

Fig. 9. Cytotoxicity data of **HQZn** (HeLa cells incubated for 24 h).

40%. The structure of **HQZn** was confirmed by ^{1}H NMR and MS spectra. The single crystal of **HQZn** grew from anhydrous Et_2O/DMF solution. The crystal structure diagrams are shown in Fig. 1. The details of the crystallographic data are listed in Table 1. As shown in Fig. 1, the crystal system of **HQZn** is monoclinic and Zn^{2+} is coordinated to three nitrogen atoms of **HQ** and two chloride ions forming a distorted square pyramidal.

3.2. UV–vis and fluorescence spectra studies

All spectroscopic measurements were carried out under simulated physiological conditions (20 mM HEPES buffer, pH = 7.4). As shown in Fig. 2, the UV–vis absorption spectra of **HQ** exhibited a maximum absorption at 355 nm in methanol–water solution. Upon increasing the amount of Zn^{2+}, the maximum absorption was gradually shifted to 394 nm along with the enhancement of intensity (Fig. 2(a)). **HQ** exhibited weak fluorescence emission at 460 nm up excitation at 400 nm (Fig. 3(a)). When saturated with Zn^{2+}, emission spectra showed a red-shift of 25 nm from 460 to 485 nm with a slight enhancement of intensity. The ratio of emission intensity ($F_{485\ nm}/F_{465\ nm}$) increased very slowly from 0.86 to 1.15 with Zn^{2+} addition (Fig. 3(b)). These confirmed the formation of the complex of **HQZn** with a molar ratio of 1:1 (**HQ**/Zn^{2+}). The red-shift of UV–vis and fluorescence spectra indicates that the nitrogen atom of the quinoline platform is coordinated with Zn^{2+} to cause an enhanced ICT process from donor (methoxy group) to acceptor (quinoline) [9,33].

Interestingly, upon the addition of Cd^{2+} to the solution of **HQZn**, the maximum absorption spectra were further shifted to 430 nm with a clear isosbestic point at 416 nm (Fig. 2(b)). The emission spectra showed a larger red-shift of 75 nm from 485 nm to 560 nm with an isoemissive point at 504 nm (Fig. 3(c)). Meanwhile, the color of the fluorescence turned from green to yellow (Fig. 3(c) inset). The ratio of emission intensity ($F_{560\ nm}/F_{485\ nm}$) increased linearly from 0.5 to 4.0 with Cd^{2+} addition and was saturated up to a molar ratio (**HQZn**/Cd^{2+}) of 1:1 (Fig. 3(d)). The further red-shift of the spectra of **HQZn** indicated that the core metal ion (Zn^{2+}) of the complex was replaced by Cd^{2+}, which further enhanced the ICT process. Job's plot analysis (Fig. 4) also confirmed the displacement. The linear enhancement of the ratio of emission intensity ($F_{560\ nm}/F_{485\ nm}$) of **HQZn** upon the addition of Cd^{2+} suggested that **HQZn** could be served as an efficient ratiometric fluorescent probe for Cd^{2+}.

Another solid evidence for displacement reaction came from the Maldi-TOF MS spectrum. As shown in Fig. 5, **HQZn** has a peak at $m/z = 481.07$ ([**HQ** + ZnCl]$^+$), upon the addition of Cd^{2+}, a peak at $m/z = 529.07$ ([**HQ** + CdCl]$^+$) appeared along with the disappearance of the peak at $m/z = 481.07$. The observations confirmed that Zn^{2+} of **HQZn** was completely displaced by Cd^{2+} to form the corresponding Cd^{2+} complex via the central metal displacement.

According to the reported method [38,39], the dissociation constants (K_d) of **HQ** for Zn^{2+} and Cd^{2+} were calculated to be 9.6 μM and 21 pM, respectively. This confirmed that Cd^{2+} exhibited higher affinity for **HQ** and can displace the Zn^{2+} of **HQZn** to form a more stable complex.

3.3. Two-photon absorption studies

Considering the application of **HQZn** in living system, we further determine the two-photon absorption cross section of **HQZn** and its corresponding Cd^{2+} complex using the two-photon induced fluorescence measurement technique. As shown in Fig. 6, the maximum two-photon absorption cross section (δ_{max}) value of

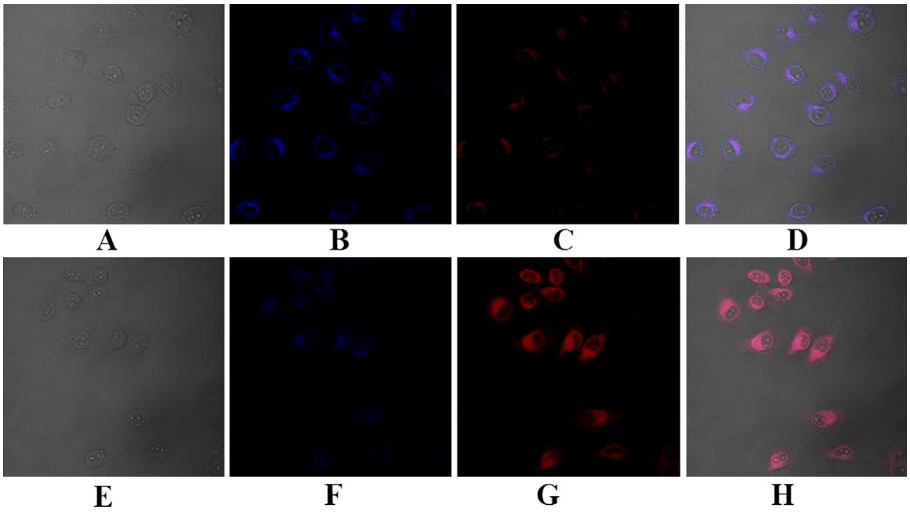

Fig. 10. (a) Bright-field image of Hela cells. (b) TP image of Hela cells disposed with 15 μM **HQZn** after 30 min of incubation, washed by PBS buffer. λ_{ex} = 730 nm (emission wavelength from 470 nm to 500 nm). (c) Emission wavelength from 545 nm to 580 nm. (d) The overlay of (a) (b) and (c). (e) Bright-field image of Hela cells. (f) TP image following a 30 min treatment with $CdCl_2$ (30 μM). Emission wavelength from 470 nm to 500 nm. (g) Emission wavelength from 545 nm to 580 nm. (h) The overlay of (e) (f) and (g).

HQZn is 48 GM at 730 nm. Upon addition of 1.2 equiv. Cd^{2+}, the δ_{max} value increases greatly to 85 GM at 730 nm. The obvious enhancement of two-photon excitation fluorescence makes **HQZn** a potential two-photon probe for monitoring Cd^{2+} flux in living systems.

3.4. Ions selectivity and pH stability

Metal ion selectivity studies were performed in HEPES buffer. As shown in Fig. 7 (black bars), Na^+, K^+, Ca^{2+}, and Mg^{2+}, which are abundant in living cells, exerted a negligible effect on the fluorescence of **HQZn** even at higher concentrations (40 times of the **HQZn**). Transition-metal ions, including Ag^+, Mn^{2+}, Cu^{2+}, Hg^{2+}, Pb^{2+}, Fe^{2+}, Co^{2+}, Ni^{2+}, Cr^{3+} and Fe^{3+} did not cause observable change of the fluorescence of **HQZn**. Competitive experiments were also carried out in presence of 1.0 equiv of Cd^{2+} mixed with 1.0 equiv of other metal ions. As shown in Fig. 7 (red bars), both alkali and transition-metal ions exert little effects on the ratiometric Cd^{2+} detecting signal ($F_{560\ nm}/F_{485\ nm}$) of **HQZn**. It's important to point out that Zn^{2+}, which often interferes the Cd^{2+} detection, causes non-change of the fluorescent spectra of **HQZn** as expected. These results suggest that **HQZn** has excellent selectivity for Cd^{2+} especially over Zn^{2+}.

Furthermore, the pH-dependence of **HQZn** and its Cd^{2+} complex was examined (Fig. 8). In the biological relevant pH range (e.g. 5–9), the ratios of fluorescence intensities at 560 nm and 485 nm ($F_{560\ nm}/F_{485\ nm}$) of **HQZn** and the corresponding Cd^{2+} complex were found to be almost pH insensitive. This indicated that pH does not affect the fluorescence signal of **HQZn** to detect Cd^{2+} under physiological conditions. Therefore, application of **HQZn** in physiological Cd^{2+} detection is possible.

3.5. Cell cytotoxicity and two-photon cell imaging

Cell cytotoxicity assays were conducted using HeLa cells to test the cytotoxicity of **HQZn**. As shown in Fig. 9, the cell viability remains more than 90% after treated with 10 μM **HQZn** for 24 h. The result indicated that **HQZn** is almost no cytotoxicity for long period incubation at low concentration and should be safe for two-photon bio-imaging.

With the above data in hand, we finally investigated the utility of **HQZn** for monitoring the intracellular Cd^{2+} flux under two-photon excitation. HeLa cells were cultured and stained with **HQZn** within 30 min and washed by PBS buffer and then treated with $CdCl_2$ another 30 min. TPM images were obtained by exciting the probe at wavelength 730 nm. The optical windows at 470–500 nm and 545–580 nm were chosen as the detecting windows for **HQZn** and **HQZn**–$\mathbf{Cd^{2+}}$. As shown in Fig. 10, before addition of Cd^{2+}, the optical window at 470–500 nm showed moderate fluorescence, whereas the optical window at 545–580 nm exhibited weak fluorescence. This indicated that **HQZn** is cell-permeable. After Cd^{2+} addition, the fluorescence of the optical window at 545–580 nm increased dramatically, whereas fluorescence of the window at 470–500 nm significantly decreased. The ratiometric fluorescence images generated from the above optical windows demonstrated that **HQZn** can reveal the variation of the intracellular Cd^{2+} flux in vivo system under two-photon excitation.

4. Conclusions

In summary, a novel Zn^{2+} complex as the ratiometric two-photon fluorescent probe (**HQZn**) for Cd^{2+} was developed. The fluorescence emission spectra of **HQZn** exhibited a large red-shift (75 nm) upon addition of Cd^{2+}. The two-photon cross section (730 nm) of **HQZn** significantly increased from 48 GM to 85 GM when the central metal ion was displaced by Cd^{2+}. Importantly, **HQZn** shows high selectivity for Cd^{2+} over other metal ions, and can eliminate the interference of Zn^{2+} during Cd^{2+} detection. Finally, in vivo two-photon microscopy imaging and cell cytotoxicity demonstrated that the new probe is cell-permeable and can be used to monitor the Cd^{2+} flux in living cells. This work may provide a new strategy to design probes for discriminating Cd^{2+} and Zn^{2+}.

Acknowledgments

This work was supported by NSFC (21102002, 21372005, 21102001, and 21272223), Natural Science Foundation of Education Department of Anhui Province (KJ2011A018), 211 Project of Anhui University and Doctor Research Start-up Fund of Anhui University for supporting the research.

Appendix A. Supplementary data

Supplementary data related to this article can be found at http://dx.doi.org/10.1016/j.dyepig.2013.09.013

References

[1] Jin T, Lu J, Nordberg M. Toxicokinetics and biochemistry of cadmium with special emphasis on the role of metallothionein. Neurotoxicology 1998;19:529–35.
[2] Satarug S, Baker JR, Urbenjapol S, Haswell-Elkins M, Reilly PE, Williams DJ, et al. A global perspective on cadmium pollution and toxicity in non-occupationally exposed population. Toxicol Lett 2003;137:65–83.
[3] Komatsu K, Urano Y, Kojima H, Nagano T. Development of an iminocoumarin-based zinc sensor suitable for ratiometric fluorescence imaging of neuronal zinc. J Am Chem Soc 2007;129:13447–54.
[4] Dodani SC, He QW, Chang CJ. A turn-on fluorescent sensor for detecting nickel in living cells. J Am Chem Soc 2009;131:18020–1.
[5] Xu ZC, Yoon J, Spring DR. A selective and ratiometric Cu^{2+} fluorescent probe based on naphthalimide excimer-monomer switching. Chem Commun 2010;46:2563–5.
[6] Choi JY, Kimb D, Yoon J. A highly selective "turn-on" fluorescent chemosensor based on hydroxyl pyrene–hydrazone derivative for Zn^{2+}. Dyes Pigment 2013;96:176–9.
[7] Zhao Q, Li RF, Xing SK, Liu XM, Hu TL, Bu XH. A highly selective on/off fluorescence sensor for cadmium(II). Inorg Chem 2011;50:10041–6.
[8] Xue L, Li GP, Liu Q, Wang HH, Liu C, Ding XL, et al. Ratiometric fluorescent sensor based on inhibition of resonance for detection of cadmium in aqueous solution and living cells. Inorg Chem 2011;50:3680–90.
[9] Lu CL, Xu ZC, Cui JN, Zhang R, Qian XH. Ratiometric and highly selective fluorescent sensor for cadmium under physiological pH range: a new strategy to discriminate cadmium from zinc. J Org Chem 2007;72:3554–7.
[10] Xu ZC, Baek KH, Kim HN, Cui JN, Qian XH, Spring DR, et al. Zn^{2+}-triggered amide tautomerization produces a highly Zn^{2+}-selective, cell-permeable, and ratiometric fluorescent sensor. J Am Chem Soc 2010;132:601–10.
[11] Peng XJ, Du JJ, Fan JL, Wang JY, Wu YK, Zhao JZ, et al. A selective fluorescent sensor for imaging Cd^{2+} in living cells. J Am Chem Soc 2007;129:1500–1.
[12] Xu L, He ML, Yang HB, Qian XH. A simple fluorescent probe for Cd^{2+} in aqueous solution with high selectivity and sensitivity. Dalton Trans 2013;42:8218–22.
[13] Tang XL, Peng XH, Dou W, Mao J, Zheng JR, Qin WW, et al. Design of a semirigid molecule as a selective fluorescent chemosensor for recognition of Cd(II). Org Lett 2008;10:3653–6.
[14] Cheng TY, Xu YF, Zhang SY, Zhu WP, Qian XH, Duan LP. A highly sensitive and selective off-on fluorescent sensor for cadmium in aqueous solution and living cell. J Am Chem Soc 2008;130:16160–1.
[15] Bao YY, Liu B, Wang H, Du FF, Bai RK. A highly sensitive and selective ratiometric Cd^{2+} fluorescent sensor for distinguishing Cd^{2+} from Zn^{2+} based on both fluorescence intensity and emission shift. Anal Methods 2011;3:1274–6.
[16] Sumalekshmy S, Henary MM, Siegel N, Lawson PV, Wu YG, Schmidt K, et al. Design of emission ratiometric metal-ion sensors with enhanced two-photon cross section and brightness. J Am Chem Soc 2007;129:11888–9.
[17] Xue L, Liu C, Jiang H. A ratiometric fluorescent sensor with a large Stokes shift for imaging zinc ions in living cells. Chem Commun 2009:1061–3.
[18] Helmchen F, Denk W. Deep tissue two-photon microscopy. Nat Methods 2005;2:932–40.
[19] Denk W, Strickler JH, Webb WW. Two-photon laser scanning fluorescence microscopy. Science 1990;248:73–6.
[20] Kim HM, Cho BR. Two-photon probes for intracellular free metal ions, acidic vesicles, and lipid rafts in live tissues. Acc Chem Res 2009;42:863–72.
[21] Zipfel WR, Williams RM, Webb WW. Nonlinear magic: multiphoton microscopy in the biosciences. Nat Methods 2003;21:1369–77.

[22] Li YM, Chong HB, Meng XM, Wang SX, Zhu MZ, Guo QX. A novel quinoline-based two-photon fluorescent probe for detecting Cd^{2+} in vitro and in vivo. Dalton Trans 2012;41:6189–94.
[23] Liu YY, Dong XH, Sun J, Zhong C, Li BH, You XM, et al. Two-photon fluorescent probe for cadmium imaging in cells. Analyst 2012;137:1837–45.
[24] Anthemidis AN, Karapatouchas CP. Flow injection on-line hydrophobic sorbent extraction for flame atomic absorption spectrometric determination of cadmium in water samples. Microchim Acta 2008;160:455–60.
[25] Goldsmith CR, Lippard SJ. 6-Methylpyridyl for pyridyl substitution tunes the properties of fluorescent zinc sensors of the zinpyr family. Inorg Chem 2006;45:555–61.
[26] Nolan EM, Lippard SJ. Small-molecule fluorescent sensors for investigating zinc metalloneurochemistry. Acc Chem Res 2009;42:193–203.
[27] Wang JL, Lin WY, Li WL. Single fluorescent probe displays a distinct response to Zn^{2+} and Cd^{2+}. Chem Eur J 2012;18:13629–32.
[28] Ravikumar I, Ghosh P. Zinc(II) and PPi selective fluorescence off-on-off functionality of a chemosensor in physiological conditions. Inorg Chem 2011;50:4229–31.
[29] Cai YL, Meng XM, Wang SX, Zhu MZ, Pan ZW, Guo QX. A quinoline based fluorescent probe that can distinguish zinc(II) from cadmium(II) in water. Tetrahedron Lett 2013;54:1125–8.
[30] An JM, Yan MH, Yang ZY, Li TR, Zhou QX. A turn-on fluorescent sensor for Zn(II) based on fluorescein-coumarin conjugate. Dyes Pigment 2013;99:1–5.
[31] Xue L, Liu Q, Jiang H. Ratiometric Zn^{2+} fluorescent sensor and new approach for sensing Cd^{2+} by ratiometric displacement. Org Lett 2009;11:3454–7.
[32] Chen XY, Shi J, Li YM, Wang FL, Wu X, Guo QX, et al. Two-photon fluorescent probes of biological Zn(II) derived from 7-hydroxyquinoline. Org Lett 2009;11:4426–9.
[33] Meng XM, Wang SX, Li YM, Zhu MZ, Guo QX. 6-Substituted quinoline-based ratiometric two-photon fluorescent probes for biological Zn^{2+} detection. Chem Commun 2012;48:4196–8.
[34] Wang SX, Meng XM, Zhu MZ. A naked-eye rhodamine-based fluorescent probe for Fe(III) and its application in living cells. Tetrahedron Lett 2011;52:2840–3.
[35] Cui X, Li J, Zhang ZP, Fu Y, Liu L, Guo QX. Pd(quinoline-8-carboxylate)$_2$ as a low-priced, phosphine-free catalyst for Heck and Suzuki reactions. J Org Chem 2007;72:9342–5.
[36] Reynolds GA, Drexhage KH. New coumarin dyes with rigidized structure for flashlamp-pumped dye lasers. Opt Commun 1975;13:222–5.
[37] Albota MA, Xu C, Webb WW. Two-photon fluorescence excitation cross sections of biomolecular probes from 690 to 960 nm. Appl Opt 1998;37:7352–6.
[38] Maruyama S, Kikuchi K, Hirano T, Urano Y, Nagano T. A novel, cell-permeable, fluorescent probe for ratiometric imaging of zinc ion. J Am Chem Soc 2002;124:10650–1.
[39] Taki M, Desaki M, Ojida A, Iyoshi S, Hirayama T, Hamachi I, et al. Fluorescence imaging of intracellular cadmium using a dual-excitation ratiometric chemosensor. J Am Chem Soc 2008;130:12564–5.